Circular RNA circARNT2 Suppressed The Sensitivity of Hepatocellular Carcinoma Cells to Cisplatin by Targeting The miR-155-5p/PDK1 Axis

Hanqin Weng
Department of Hepato-Billiary Surgery, Dongguan people's Hospital, Southern Medical University, Dongguan
Linhui Cao
Department of Traditional Chinese Medicine, Sun Yat-sen Memorial Hospital, Sun Yat-sen University,
Xiaochun Chen
Department of Gastroenterology, Dongguan People's Hospital, Southern Medical University
Liqing Ye
Department of Hepato-Billiary Surgery, Dongguan people's Hospital, Southern Medical University
Weijian Feng
Department of Hepato-Billiary Surgery, Dongguan people's Hospital, Southern Medical University
Liping Li
Department of Hepato-Billiary Surgery, Dongguan people's Hospital, Southern Medical University
Yibiao Ye
Department of Hepato-Billiary Surgery, Sun Yat-sen Memorial Hospital, Sun Yat-sen University
Zaiguo Wang (drzhangtc66@163.com)
Department of Hepato-Billiary Surgery, Dongguan people's Hospital, Southern Medical University. Dongguan

Research

Keywords: CircARNT2, CircRNA, HCC, Chemoresistance, Cisplatin, CeRNA, miR-155-5p.

Posted Date: July 7th, 2020

DOI: https://doi.org/10.21203/rs.3.rs-39627/v1

Abstract

Background: Circular RNA (circRNA) is a novel subclass of noncoding-RNA molecules that participate in development and progression of a variety of human diseases via sponging microRNAs (miRNAs). Until now, the contributions of circRNAs in chemoresistance of hepatocellular carcinoma (HCC) remain largely unknown.

Methods: In the present study, we aimed to investigate the role of circRNA in cisplatin resistance of HCC. We investigated the expression of circRNAs in 5 paired cisplatin-sensitive and cisplatin-resistant HCC tissues by microarray analysis. The qRT-PCR analysis was to investigate the expression pattern of circARNT2 in HCC patient tissues and cell lines. Then, the effects of circARNT2 on cisplatin resistance, cell proliferation, and apoptosis were assessed in HCC *in vitro* and *in vivo*.

Results: CircARNT2 was significantly upregulated in HCC tissues and cell lines. Overexpression of circARNT2 in HCC was significantly correlated with aggressive characteristics and served as an independent risk factor for overall survival in patients with HCC. *In vitro* experiments showed that knockdown of circARNT2 inhibited cell proliferation and enhances the cisplatin sensitivity of HCC cells. Furthermore, circARNT2 facilitates HCC progression *in vivo*. We demonstrated that circARNT2 acts as a sponge for miR-155-5p and verified that PDK1 is a novel target of miR-155-5p.

Conclusion: In summary, our study demonstrated that circARNT2 modulates cisplatin resistance through miR-155-5p/PDK1 pathway. Our findings indicated that circARNT2 may serve as a promising therapeutic target for overcoming cisplatin resistance for HCC.

Background

Hepatocellular carcinoma (HCC) is the most common neoplasm of primary liver cancers, accounting for 85–90% of all cases [1]. HCC is mainly associated with chronic liver disease and cirrhosis [2]. The treatment options for advanced-stage HCC are very limited. HCC can be treated with liver transplantation, surgical resection, radiofrequency ablation, transcatheter arterial chemoembolization and systemic chemotherapy [3]. Because of late-stage detection and lack of effective therapies, the majority of patients lose the opportunity for surgery [4]. Despite advances of modern treatments, chemotherapy is still a main and effective approach to control the development of HCC and prolong patients' life [5]. However, many HCC cases show poor response to chemotherapy [6,7]. Chemoresistance is still a major obstacle for HCC patients to obtain a satisfactory curative effect. Thus, identifying new targets for therapeutic intervention and developing novel diagnostic approaches are in great need for early diagnosis and intervention for HCC.

Circular RNA (circRNA) is a novel type of noncoding RNA with a covalently closed loop, which is generated by the back-splicing of pre-mRNA [8]. More newly identified circRNAs have been found using high-throughput sequencing and via further functional validation [9]. Increasing evidences indicate that

circRNAs are implicated in several pathophysiological processes including human cancers [10,11]. Aberrant expression of circRNAs has been frequently observed in cancers [12,13]. Moreover, circRNAs regulate malignant behaviors of cancer cells, such as proliferation, apoptosis resistance, migration, invasion and drug resistance [14,15]. Although several circRNAs have been reported to participate in the tumorigenesis and progression of HCC [16–18], the expressions and roles of circRNA in chemoresistance of HCC remains unclear.

In this study, we aimed to investigate the role of circRNA in cisplatin resistance of HCC. We identified 968 significantly dysregulated circRNAs in cisplatin-resistant HCC tissues. We focused on hsa_circ_0104670, which is located on chr15:80767350–80772264 and derived from ARNT2 gene, and thus we termed as circARNT2. We further tested circARNT2 in HCC samples by qRT-PCR and the results showed that the expression of circARNT2 was markedly elevated both in HCC tissues and exosomes from HCC plasma. Gain-offunction investigations showed that circARNT2 overexpression suppressed cancer cell growth *in vivo* and *in vitro*. Subsequent studies displayed that circARNT2 could sensitize HCC cells to cisplatin by targeting the miR-155-5p/PDK1 signaling axis. Our findings will provide new insights into the regulatory mechanisms of circARNT2 in tumor progression and cisplatin resistance of HCC.

Materials And Methods

Clinical specimens

A total of 82 pairs of HCC and tumor-adjacent tissues were collected from patients who underwent hepatectomy at Department of Hepato-Billiary Surgery, Sun Yat-sen Memorial Hospital, Sun Yat-sen University. None of HCC patients received any pre-operative treatments. The tissue samples were confirmed by two histopathologists. All samples were immediately snap-frozen in liquid nitrogen and subsequently stored at - 80 °C until RNA extraction. The research has been carried out in accordance with the World Medical Association Declaration of Helsinki.

Ethical approval was obtained from the Sun Yat-sen Memorial Hospital, Sun Yat-sen University Research Ethics Committee, and written informed consent was obtained from each patient.

Cell culture

HCC cell lines Hep3B, Huh-7 and the normal human liver cell line LO2 were purchased from the Chinese Academy of Sciences Cell Bank Type Culture Collection. The cells were cultured with DMEM and RPMI-1640 (Gibco, Carlsbad, CA) together with 10% fetal bovine serum (Gibco) at 37°C in an atmosphere containing 5% CO_2. The cisplatin-resistant Hep3B (Hep3B-R) and Huh7 (Huh7-R) cells were prepared according to the method previously described[19].

CircRNA microarray analysis

Total RNA was extracted from patients with cisplatin-resistant or cisplatin-sensitive HCC using the RNeasy Mini Kit (Qiagen, GmBH, Hilden, Germany) according to the manufacturer's instructions. The adjacent tissues were used as control. Patients with cisplatin-resistant HCC were defined as those with persistent disease more than two months, and those with recurrent disease more than 2 months after completion of chemotherapy containing cisplatin. Patients with cisplatin-sensitive HCC were defined as those without local residual lesions or recurrence at 2 months after completion of chemotherapy containing cisplatin. Purified total RNA was quantified using the NanoDrop 2000 spectrophotometer. The total RNA was sent to Aksomics Co. Ltd. (Shanghai, China) to analyze circRNA expression profiles. Differentially expressed circRNAs were identified as fold change > 2 and adjusted $p < 0.05$.

TCGA dataset analysis

The data and the corresponding clinical information of patients were collected from the Cancer Genome Atlas (TCGA) database (http:// cancergenome.nih.gov/). We used the edgeR package of R packages to perform the difference analysis (http://www. bioconductor.org/packages/release/bioc/html/edgeR.html) and used the pheatmap package of R packages to perform the cluster analysis (https://cran.r-project.org/web/packages/pheatmap/ index.html). Sva R package was used to remove the batch effect. Genes with adjusted p values < 0.05 and absolute fold changes (FC) > 1.5 were considered differentially expressed genes. Kaplan–Meier survival curves were drawn to analyse the relationships between genes and overall survival in the survival package. The corresponding statistical analysis and graphics were performed in R software (R version 3.3.2).

RNA Isolation and qRT-PCR

RNA was totally extracted from the cells and tissue using the with TRIzol reagent (1 mL) (Invitrogen) based on the manufacturer's protocol. The testing for miRNA extraction was mirVana miRNA isolation kit (Ambion, Austin, TX, USA). After isolation, the RNA concentration in the RNA solution was determined using Nano- Drop 1000 spectrophotometer (Thermo Scientific, Wilmington, DE, USA) and stored at 80°C for further use. Glyceraldehyde-3- phosphate dehydrogenase (GAPDH) was used as an endogenous control.

SiRNA and plasmid construction and cell transfection

For transfections, cells at the confluence of 50–80% were infected with 1×10^6 recombinant lentivirus-transducing units and 6 μg/mL Polybrene (Sigma, Shanghai, China). Stably transfected cells were selected via treatment with 2μg/mL puromycin for 2 weeks. Stably transfected cells were picked via flow cytometry for subsequent assays. Plasmid, lentivirus, miRNA inhibitor and miRNA mimics used in this study were purchased from GenePharma Co., Ltd. (Shanghai, China), pHBV1.3 copy was purchased from Miaolingbio (Wuhan, China). Lipofectamine 3000 (Invitrogen, CA, USA) was utilized for transfection.

CCK-8assay

After transfection, the cells mixed with 10 ml of CCK-8 solutions per well and incubated for further 1 h at 37 °C. The amount of formazan dye generated by cellular dehydrogenase activity was measured for absorbance at 450nm by a microplate reader (Molecular Devices, Sunnyvale, CA, USA). The optical density values of each well represented the survival/proliferation of HCC cells.

Flow cytometric analysis

Transfected cells were harvested after transfection by trypsinization. After the double staining with fluorescein isothiocyanate (FITC)-Annexin V and propidium iodide was done by the FITC Annexin V Apoptosis Detection Kit (BD Biosciences) according to the manufacturer's recommendations, the cells were analyzed with a flow cytometry (FACScan; BD Biosciences) equipped with a Cell Quest software (BD Biosciences). Cells were discriminated into viable cells, dead cells, early apoptotic cells, and apoptotic cells and then the relative ratio of early apoptotic cells were compared with control transfection from each experiment.

Tumor xenograft in nude mice

Ten nude mice (5 mice per group, male, 2 months old) were purchased from Shanghai Experimental Animal Center (Shanghai, China). Mice were subcutaneously injected into the back with 1×10^6 SR-HepG2 cells transfected with si-circARNT2 or si-NC suspended in 100 μL Hank's balanced salt solution. The tumor size was measured every 3 days with a caliper, and tumor volume was calculated according to the formula: volume = length × width^2/2. All mice were killed by cervical dislocation on day 21 after inoculation. The resected tumor masses were harvested for subsequent weight and qRT-PCR analysis. Animal experiments were approved by the Ethical Committee for Animal Research of the Sun Yat-sen Memorial Hospital, Sun Yat-sen University. The animal work has taken place in the animal central of Sun Yat-sen Memorial Hospital, Sun Yat-sen University.

Immunohistochemistry

The expression of Ki67 in tumor tissues from nude mice was analyzed by immunohistochemical analysis. Briefly, the tissues were fixed with 4% formaldehyde for 24 h, embedded and cut into 4-μm-thick section. The sections were treated with 10 mmol/l sodium citrate buffer and incubated with anti-Ki67(1: 200 dilution) and anti-PDK1 antibody (1: 200 dilution) overnight at 4 °C. The positive signaling was stained by using a Mouse and Rabbit Specific HRP/DAB (ABC) Detection IHC kit (Abcam Trading (Shanghai) Company Ltd., Shanghai, China), and counterstained with hematoxylin. The relative integral optical density (IOD) of positive signaling was obtained by ImageJ software.

Actinomycin D and RNase R treatment

To block transcription, 2 mg/ml Actinomycin D or dimethylsulphoxide (Sigma-Aldrich, St. Louis, MO, USA) as a negative control was added into the cell culture medium. For RNase R treatment, total RNA (2 μg) was incubated for 30 min at 37 °C with or without 3 U/μg of RNase R (Epicentre Technologies, Madison,

WI, USA). After treatment with Actinomycin D and RNase R, qRT-PCR was performed to determine the expression levels of circARNT2 and ARNT2 mRNA.

Isolating RNAs from nucleus and cytoplasmic fractions

The nuclear and cytoplasmic fractions were isolated using PARIS™ Kit (Invitrogen, Carlsbad, CA, USA) following the manufacture's protocol. Briefly, cells were collected and lysed with cell fractionation buffer, followed by centrifugation to separate the nuclear and cytoplasmic fractions. The supernatant containing the cytoplasmic fraction was collected, and transferred to a fresh RNase-free tube. The nuclear pellet was lysed with Cell Disruption Buffer. The cytoplasmic fraction and nuclear lysate were mixed with 2X Lysis/Binding Solution and then added with 100% ethanol. The sample mixture was drawn through a Filter Cartridge, followed by washing with Wash Solution. The RNAs of nuclear and cytoplasmic fractions were eluted with Elution Solution. U6 snRNA and 18S rRNA were employed as positive control for nuclear and cytoplasmic fractions, respectively.

Western blot analysis

The cells were lysed using RIPA protein extraction reagent (Beyotime, Beijing, China) supplemented with a protease inhibitor cocktail and phenylmethylsulfonyl fluoride (Roche, Basel, Switzerland). Protein concentration was measured using the Bio-Rad protein assay kit. Approximately 50 μg of protein extract was separated by 10% SDS-polyacrylamide gel electrophoresis (SDS-PAGE), then transferred to nitrocellulose membrane (Sigma) and incubated with specific antibodies. ECL chromogenic substrate was used to visualize the bands and the intensity of the bands was quantified by densitometry (Quantity one software; Bio-Rad, Hercules, CA, USA). GAPDH was used as a control. Primary antibodies against PDK1 (Abcam, ab13755) was purchased from Abcam and used in a 1:1000 dilution in 5% BSA.

Biotin-coupled miRNA capture

Briefly, the 30 end biotinylated miR-RNA mimic or control biotin-RNA (RiboBio) was transfected into SPC-A1 cells at a final concentration of 20 nmol/L for 1 day. The biotin-coupled RNAcomplex was pulled down by incubating the cell lysate with streptavidin-coated magnetic beads (Ambion, Life Technologies).

Luciferase reporter assays

The luciferase reporter assays were carried out with the help of the Dual-luciferase Reporter Assay System (Promega, Madison, WI, USA). The wide-type circARNT2 or mutant circARNT2 that had the predicted miR-155-5p binding site was established and integrated into a pmir-GLO Dual-luciferase vector to form the pmirGLO-circARNT2-wild type (circARNT2-wt) or pmirGLO-circARNT2-mutant (circARNT2-mut) reporter vector. Cotransfection of circARNT2-wt or circARNT2-mut was carried out with miR-155-5p mimics or negative control into HCC cells with the use of Lipofectamine 2000. Subsequent to transfection for a period of 48 hours, the luciferase activities were measured in accordance with the guidelines of the manufacturer. In the same manner, pmirGLO-PDK1-wild type (PDK1-wt) or pmirGLO-PDK1-mutant (PDK1-

mut) were constructed, together with cotransfecting with miR-155-5p mimics or negative control into cells. 48 hours following the transfection, the relative luciferase activities were detected.

RNA immunoprecipitation (RIP)

Magna RIP™ RNA-Binding Protein Immunoprecipitation Kit (Millipore, Billerica, MA, USA) were used for RIP. Cells were lysed in complete RNA lysis buffer, then cell lysates were incubated with RIP buffer containing magnetic beads conjugated with human anti-Argonaute2 (AGO2) antibody (Millipore) or negative control mouse IgG (Millipore).

Immunofluorescence and confocal imaging

Cells were fixed with 4% paraformaldehyde and permeabilized by 1% Triton X-100. After blocking with 1% bovine serum albumin, cells were serially incubated with rabbit anti-P62 (Abcam) and Goat antirabbit Alexa Fluo488 (Invitrogen). Images were acquired using the AV300-ASW confocal microscope (Olympus America Inc., Center Valley, USA) with a 60×oil lens. Pictures were analyzed using Image- Pro Plus 6.0 (Media Cybernetics).

Statistical analysis

Results are presented expressed as mean±SD (standard deviation). Student's t test was performed to measure the difference between two group and differences between more than two groups were assessed using one-way ANOVA. $P<0.05$ was considered significant.

Results

Upregulation of circARNT2 is associated with cisplatin resistance in HCC

To investigate the role of circRNAs in cisplatin resistance of HCC, we performed circRNAs array to identify the differentially expressed circRNAs. A total of 9857 circRNAs were detected in 5 pairs of cisplatin-resistant HCC tissues and cisplatin-sensitive HCC tissues by the circRNA microarray analysis. Among them, 968 circRNAs were significantly aberrantly expressed ($P < 0.05$ and fold-change > 2.0) between cisplatin-resistant HCC tissues and cisplatin-sensitive HCC tissues. Of these circRNAs, 538 were significantly upregulated and 430 were significantly downregulated in cisplatin-resistant HCC tissues compared with cisplatin-sensitive HCC tissues. Among the 968 differentially expressed circRNAs, 246, including 132 upregulated ones and 114 downregulated ones, were verified as novel circRNAs; 722 circRNAs, including 406 upregulated and 316 downregulated ones, had been identified beforehand and listed in the circRNA database (circBase; http://www.circbase.org) (Fig.1A). The 968 identified circRNAs were divided into five different categories on the basis of the way they were produced. Exonic circRNAs consisting of the protein-encoding exons accounted for 70.97% (687/968), intronic circRNAs from intron lariats comprised 8.99% (87/968), sense overlapping circRNAs that originated from exon and other sequence circRNAs comprised 18.08% (1555/968), intergenic circRNAs composed of unannotated sequences of the gene and antisense circRNAs originating from antisense regions equally comprised

1.96% (19/968) (Fig.1B). Hierarchical clustering was then performed to demonstrate the five most upregulated circRNAs (hsa_circ_0005394, hsa_circ_0001741, hsa_circ_0006916, hsa_circ_0102034, and hsa_circ_0104670) and five most downregulated circRNAs (hsa_circ_0000567, hsa_circ_0004058, hsa_circ_0001649, hsa_circ_0103809, and hsa_circ_0004018) expression patterns among the sets (Fig. 1C).

The five most upregulated circRNAs were selected and validated by qRT-PCR using 82 HCC and paired non-tumorous tissue samples. As shown in Fig. 1D-H, qPCR results further confirmed that circ_0104670 was significantly increased in HCC tissues compared with adjacent tissues, and its expression was higher in cisplatin-resistant HCC tissues than in the cisplatin-sensitive tissues. By browsing the human reference genome (GRCh37/hg19), we identified that hsa_circ_0104670 (chr15:80767350-80772264) is derived from ARNT2, with a spliced mature sequence length of 4914 base pairs (bp), and thus we named it circARNT2. We verified its existence in many circRNA databases. According to the circBase database, circARNT2 is detected in normal human frontal_cortex (http://www.circbase.org/cgi-bin/singlerecord.cgi?id=hsa_circ_0104670).

To further investigate the role of circARNT2 in HCC, the relationship between circARNT2 expression in HCC tissues and clinicopathological characteristics of HCC patients was analysed. Using the median expression level of circARNT2 as cutoff value, patients who expressed circARNT2 equal to or greater than the average level were assigned to the “circARNT2 high” group. As shown in Table 1, high expression of circARNT2 in HCC tissues was significantly correlated with tumor size (P= 0.003), distant metastasis (P= 0.031) and TNM stage (P= 0.023) but not related to gender, age and differentiation. In addition, further Kaplan–Meier survival analyses revealed that the HCC patients with high circARNT2 level had shorter overall survival than the patients had low circARNT2 level (P = 0.012, Fig. 2A). We also found that circARNT2 was significantly increased in cisplatin resistant HCC cell lines (Hep3B-R and Huh7-R) compared with the parental HCC cell lines (P < 0.01; Fig. 2B). These results suggest that circARNT2 is closely associated with cisplatin resistance in HCC.

CircARNT2 regulates the cisplatin chemosensitivity of HCC *in vitro*

To further validate the expression level of circARNT2 on cisplatin resistance, circARNT2 shRNA and circARNT2 overexpression vector were constructed, and we performed loss- and gain-of-function studies by knocking down or overexpressing circARNT2 in HCC cells. Firstly, we knocked down the expression of both circARNT2 and ARNT2 mRNA. Hep3B-R and Huh7-R cells were transfected with three kinds of circARNT2 shRNA (respectively sh-circARNT2 #1, sh-circARNT2 #2, or sh-circARNT2#3) or GFP lentivirus (sh-CTL), and the sequence only in the linear transcript (si-ARNT2). As expected, shRNA directed against the backsplice sequence knocked down only the circular transcript and did not affect the expression of linear species, and siRNA targeting the sequence in the linear transcript knocked down only the linear transcript and did not affect the expression of the circular transcript in Hep3B-R and Huh7-R cells (Figure S1A-F; P < 0.01). Due to the highest efficiency of interference, sh-circARNT2 #3 was chosen for the subsequent experiments. Meanwhile, we infected Hep3B and Huh7 cells with the circARNT2

overexpression adenovirus (circARNT2 OE) or control GFP adenovirus (circARNT2 CTL). The qRT-PCR assay indicated the relative abundance of circARNT2 in Hep3B and Huh7 cells infected with adenovirus (Fig. S1G and H; $P < 0.01$). We found that inhibition of circARNT2 significantly inhibited cells proliferation (Fig. 2C-D) and induced apoptosis (Fig. 2E-F) in Hep3B-R and Huh7-R cells compared with negative control. In addition, circARNT2 downregulation sensitized Hep3B-R and Huh7-R cells to cisplatin (Fig. 2G-H).

CircARNT2 knockdown inhibited the growth of HCC*in vivo*

Furthermore, the tumor suppressive effects of circARNT2 downregulation were also confirmed *in vivo*. Hep3B-R cells stably infected with sh-circARNT2 or sh-CTL were subcutaneously injected into each mouse. Our results showed that the tumor volumes in nude mice injected with sh-circARNT2-transfected Hep3B-R cells were smaller than in the control nude mice (Fig. 3A). Tendencies in tumor weight were consistent with those in tumor volume (Fig. 3B). The proliferative marker ki67 expression was decreased in tumor tissues of nude mice injected with sh-circARNT2-transfected Hep3B-R cells (Fig. 3C-D).

Confirmation of the circular structure and subcellular localization of circARNT2

Next, we investigated the stability and localization of circARNT2 in HCC cells. Total RNAs from Hep3B-R and Huh7-R cells were isolated at the indicated time points after treatment with Actinomycin D, an inhibitor of transcription. Then qRT-PCR was performed to measure the level of circARNT2 and ARNT2 mRNA. The results showed that the halflife of circARNT2 exceeded 24 h, whereas that of circARNT2 mRNA was about 4 h in both Hep3B-R and Huh7-R cells (Fig. 4A-B). Furthermore, we found that circARNT2 was resistant to RNase R digestion (Fig. 4C-D). These data confirmed that circARNT2 was a circular RNA. We then investigated the localization of circARNT2. The qRT-PCR of RNAs from nuclear and cytoplasmic fractions indicated that circARNT2 was predominantly localized in the cytoplasm of Hep3B-R and Huh7-R cells (Fig. 4E-F). Collectively, the above data suggested that circARNT2 harbored a loop structure and was predominantly localized in the cytoplasm.

CircARNT2 functioned as a molecular sponge of miR-155-5p in HCC cells

Given that many circRNAs can function as miRNA sponges in the cytoplasm, we determined whether circARNT2 may also bind to miRNAs as a sponge and regulate targets via the competitive endogenous RNA (ceRNA) mechanism. We therefore analyzed the sequence of circARNT2 using the miRanda algorithm and identified 199 miRNA-binding sites (Table S1); however, five miRNAs with relatively high scores (miRNA-155-5p, miRNA-1197, miRNA-155-5p, miRNA-1228, and miRNA-1236) were finally selected.

It is well known that miRNAs usually silence gene expression by combining with the AGO2 protein and form the RNA-induced silencing complex (RISC). In the context of ceRNA mechanism, it might be a prevalent phenomenon that AGO2 could bind with both circRNAs and miRNAs. We therefore conducted an RIP assay to pull down RNA transcripts that bind to AGO2 in Hep3B-R cells. Indeed, endogenous circARNT2 was efficiently pulled down by anti-Ago2 (Fig. 5A). To further detect whether circARNT2 could

sponge miRNAs, we performed a miRNA pull-down assay using biotin-coupled miRNA mimics (miRNA-155-5p, miRNA-1197, miRNA-155-5p, miRNA-1228, and miRNA-1236). Interestingly, circARNT2 was only efficiently enriched by miR-155-5p, but not by the other three miRNAs (Fig. 5B). In order to further validate the interaction, circARNT2 sequence containing the putative or mutated miR-155-5p binding site was cloned into the downstream of luciferase reporter gene, generating WT-circARNT2 or MUT-circARNT2 luciferase reporter plasmids. Then the effect of miR-155-5p on WT-circARNT2 or MUT-circARNT2 luciferase reporter systems was determined. The results showed that miR-155-5p mimic considerably reduced the luciferase activity of the WT-circARNT2 luciferase reporter vector compared with negative control, while miR-155-5p mimic did not pose any impact on the luciferase activity of MUT-circARNT2-transfected Hep3B-R cells (P<0.01, Fig. 5C). In a further RIP experiment, circARNT2 and miR-155-5p simultaneously existed in the production precipitated by anti-AGO2 (P<0.01, Fig. 5D), suggesting that miR-155-5p is circARNT2-targeting miRNA. Furthermore, silencing of circARNT2 did not affect the expression of miR-155-5p, and transfection of miR-155-5p mimics did not affect the expression of circARNT2 (Fig. 5E and F), which indicated circARNT2 functions as a miRNA sponge without affecting the expression of sponged miRNAs.

MiR-155-5psuppressed cisplatin-resistant HCC tissues resistance of HCC cells

The qRT-PCR analysis indicated that there was a decreasing trend in miR-155-5p levels from normal liver tissues to cisplatin-sensitive HCC tissues and then to cisplatin-resistant HCC tissues, and the differences among the three groups were significant (P<0.01, Fig. 6A). We also confirmed that the expression of miR-155-5p was obviously decreased in cisplatin resistant cells than that in cisplatin sensitive cells, indicating the opposite result to circARNT2 expression (P<0.01, Fig. 6B). To gain insight into whether circARNT2 affected cisplatin resistance of HCC cells via modulation of miR-155-5p, we further performed rescue assays to confirm how miR-155-5p modulated cisplatin resistance. We transfected miR-155-5p mimics or inhibitors into HCC cells and the proliferation curves were performed. Our results showed that Hep3B cells transfected with miR-155-5p inhibitors grew at a dramatically higher rate as compared with controls (Fig. 6C; P < 0.01), whereas miR-155-5p mimics markedly inhibits the cell growth in Hep3B-R cells when compared with cells transfected with miR-NC (Fig. 6D; P < 0.01). Moreover, cell proliferation assay proved that downregulation of circARNT2 markedly inhibits the cell growth of Hep3B-R cells, whereas sh-circARNT2#3-induced decrease of cell growth was partially restored by miR-155-5p inhibition (Fig. 6E; P < 0.01). Furthermore, flow cytometry analysis indicated that circARNT2 knockdown dramatically aggravated cisplatin-induced apoptosis of Hep3B-R cells, however, sh-circARNT2#3-triggered apoptosis was attenuated after cotransfected with miR-155-5p inhibitor (Fig. 6F; P < 0.01). Together, these data hinted that inhibition of miR-155-5p could significantly reversed circARNT2-mediated cisplatin resistance in HCC cells.

MiR-155-5p inhibits PDK1 and promotes autophagy

We sought to explore potential target genes of miR-155-5p. Bioinformatics analysis by using the TargetScan and Findtar algorithm predicted one putative and highly conserved miR- 155-5p binding site

within the 3'UTR of PDK1 (Fig. 7A). Then, we focused on the transcriptional regulation of PDK1 expression by miR-155-5p. We constructed a luciferase reporter gene plasmid containing PDK1 wild-type 3'-UTR and its mutant 3'-UTR (Fig. 7A). The dual luciferase reporter gene assay showed that the fluorescence enzyme activity was significantly decreased after co-transfection with the PDK1 wild-type 3'-UTR construct and miR-155-5p mimics. In contrast, the fluorescence enzyme activity was nearly unchanged after co-transfection with PDK1 mutant 3'-UTR construct and miR-155-5p mimics (Fig. 7B). To determine the expression levels of PDK1 in HCC, we analysed the PDK1 expression in the HCC tissues. The immunohistochemistry results showed that PDK1 expression in HCC specimens was significantly upregulated compare with that in the adjacent normal tissues ($P<0.001$; Fig. 7C). To further confirm the effects of circARNT2 on PDK1 expression, HCC cells were transfected with the circARNT2 siRNA, and the PDK1 protein levels were detected using western blotting. The results showed that knockdown of circARNT2 expression significantly reduced the PDK1 protein levels in SR-HepG2 cells (Fig. 7D). Moreover, inhibition of circARNT2 mediated decrease of PDK1 protein expression was significantly recuperated following miR-155-5p inhibitors (Fig. 7D).

Previous studies have shown that PDK1 is a critical checkpoint for autophagy dysfunction. To determine the role of miR-155-5p in autophagy, we transfected miR-155-5p mimics into Hep3B-R cells and performed the immunofluorescence assay. We found that the expression levels P62, a marker of autophagy, was significantly reduced in miR-155-5p-overexpressing cells compared to the corresponding control cells (Fig. 7E). Taken together, the results indicate that autophagy activity could be enhanced with upregulation of miR-155-5p expression. Taken together, our results indicate that circARNT2 positively regulated PDK1 expression by interacting with miR-155-5p, and this is then followed by the inhibition of autophagy.

Discussion

In this study, we explored the effect of circARNT2 on the chemosensitivity of HCC and demonstrate the regulatory mechanism of miR-155-5p/PDK1 signaling pathway. We first discovered that circARNT2 is frequently upregulated in HCC, and its expression significantly correlated with poor clinicopathologic characteristics. Second, our data showed that the high expression of circARNT2 correlated with poor patient prognosis, indicating its applicability as a promising prognostic biomarker in HCC. Third, we demonstrated that the inhibition of circARNT2 reversed the cisplatin resistance of HCC cells and thus inhibited the progression of HCC. Fourth, we revealed that circARNT2 acts as a ceRNA and regulates PDK1-induced autophagy by competing for miR-155-5p. These results suggested that circARNT2 may have the potential to regulate the cisplatin resistance of HCC, in turn promoting the progression of HCC.

In the last decade, improved drug therapy agents have significantly prolonged the survival of HCC patients with advanced diseases [19]. Cisplatin, the first-generation of the platinum chemotherapeutic drugs, can inhibit DNA replication and transcription by forming crosslinks between DNA double strands and exhibits broad-spectrum antitumor activity. Cisplatin is one of the most commonly used chemotherapeutic agents to treat advanced HCC. However, the acquisition of multi-drug resistance (MDR)

to cisplatin is still a major obstacle for HCC patients to obtain a satisfactory curative effect [20]. Recent studies have verified that many circRNAs play critical roles in modulating tumor development and progression [21]. However, the mechanisms by which circRNAs participate in HCC development and drug resistance remains unclear. Using a circRNA microarray assay, we analysed aberrantly-expressed circRNAs between cisplatin-resistant HCC tissues and cisplatin-sensitive HCC tissues. Results showed 538 were significantly upregulated and 430 were significantly downregulated in cisplatin-resistant HCC tissues compared with cisplatin-sensitive HCC tissues. Then, we demonstrated that circARNT2 was upregulated in HCC tissues and associated with cisplatin resistance in HCC. To further validate whether circARNT2 functionally required for cisplatin resistance, we performed loss-of-function studies by knockdown circARNT2 in cisplatin resistant HCC cell lines (Hep3B-R and Huh7-R). Meanwhile, we overexpressed circARNT2 in Hep3B and Huh7 cells. Loss-of-function experiments revealed that knockdown of circARNT2 inhibited the cisplatin-induced cell apoptosis and cell mobility of cisplatin-resistant cells. Gain-of-function experiments revealed that ectopic expression of circARNT2 promoted proliferation and promoted apoptosis of cisplatin sensitive cells, compared with negative control-transfected cells. In addition, xenograft experiments revealed that circARNT2 knockdown inhibited the growth of HCC *in vivo.*

CircRNAs may act as transcription regulators or as sponges for small RNA regulators, which compete for microRNA (miRNA) activity in the process of regulating cell proliferation [22]. Most circRNAs have miRNA-binding sites that can be used as miRNA sponges to inhibit the regulation of miRNAs on downstream target genes by a large number of miRNAs in cancers [23]. Herein, circARNT2 has been shown to target miRNA-155-5p using bioinformatics tools. Intriguingly, the ectopic expression of miRNA-155-5p reduced the luciferase activity of the wt-circARNT2 reporter. However, there was no significant difference in circARNT2 expression upon forced miRNA-155-5p expression. Furthermore, endogenous circARNT2 and miRNA-155-5p were pulled down by a special AGO2 antibody. Ultimately, we found that circARNT2 enhances the cisplatin resistance, mainly through interaction with miRNA-155-5p, and miRNA-155-5p mimics reversed circARNT2-mediated cisplatin resistance effects. Taken together, all of the data suggest that miRNA-155-5p recognizes and binds to circARNT2 without promoting the degradation of circARNT2.

In this study, we identified circARNT2 as a new interactive molecule of miRNA-155-5p, also confirmed that PDK1 was a new downstream target of miRNA-155-5p. PDK1 is now widely studied in malignant tumors because PDK1 can serve as an important junction point for multiple cell signaling pathways [24]. The immunohistochemistry results showed that PDK1 expression in HCC specimens was significantly upregulated compare with that in the adjacent normal tissues. CircARNT2 could control the PDK1 level by provoking miRNA-155-5p. Previous studies have shown that PDK1 is a critical checkpoint for autophagy dysfunction [25]. Autophagy is an important metabolic process for maintaining cell homeostasis. Autophagy reduces protein synthesis and increases protein degradation, thereby inhibiting the proliferation of primary cancer cells and tumor growth [26]. We found that the expression of miR-155-5p contrasted with the activity of autophagy marker protein (P62), indicating that upregulation of miR-155-5p induces autophagy in HCC cells.

Conclusion

In conclusion, our study revealed that circARNT2 is frequently activated in cisplatin-resistant HCC tissues and cell lines and associated with a poor survival outcome. These results indicate that circARNT2 functions as an oncogene by sponging miR-155-5p, leading to PDK1 upregulation, and finally promotes autophagy and sensitizes HCC cells to cisplatin. Therefore, our findings provide significant evidence to further elucidate the therapeutic use of circRNA in HCC.

List Of Abbreviations

circRNAs: Circular RNAs; circARNT2: Circular RNA ARNT2; microRNAs: miRNAs; HCC: Hepatocellular carcinoma; MVI: Microvascular invasion; OS: Overall survival; qRTPCR: Quantitative real-time PCR; RIP: RNA immunoprecipitation;

Declarations

Ethics approval and consent to participate

The research has been carried out in accordance with the World Medical Association Declaration of Helsinki. Ethical approval was obtained from the Sun Yat-sen Memorial Hospital, Sun Yat-sen University Research Ethics Committee, and written informed consent was obtained from each patient.

Consent for publication

We have received consents from individual patients who have participated in this study. The consent forms will be provided upon request.

Availability of data and materials

The datasets used and analysed during the current study are available from. the corresponding author on reasonable request.

Competing interests

The authors declare that they have no competing interests.

Funding

Provincial basic and applied basic research project (provincial natural fund) Doctor start up project. No. 2016A030310089.

Authors' contributions

Hanqin Weng and Zaiguo Wang performed primers design and experiments. Linhui Cao and Xiaochun Chen contributed flow cytometry assay and animal experiments. Liqing Ye and Weijian Feng collected and classified the human tissue samples. Liping Li and Yibiao Ye contributed to qRT-PCR. Zaiguo Wang analyzed the data. Hanqin Weng wrote the paper. All authors read and approved the final manuscript.

Acknowledgements
Not applicable.

References

1. Bray F, Ferlay J, Soerjomataram I, Siegel RL, Torre LA, Jemal A. Global cancer statistics 2018: GLOBOCAN estimates of incidence and mortality worldwide for 36 cancers in 185 countries. CA Cancer J Clin 2018.
2. Chan AWH, Zhong J, Berhane S, Toyoda H, Cucchetti A, Shi K, Tada T, et al. Development of pre and post-operative models to predict early recurrence of hepatocellular carcinoma after surgical resection. J Hepatol 2018.
3. Yang JD, Roberts LR. Hepatocellular carcinoma: A global view. Nat Rev Gastroenterol Hepatol. 2010;7:448–58.
4. El-Serag HB, Marrero JA, Rudolph L, Reddy KR. Diagnosis and treatment of hepatocellular carcinoma. Gastroenterology. 2008;134:1752–63.
5. El-Serag HB. Hepatocellular carcinoma. N Engl J Med. 2011;365:1118–27.
6. Harlan LC, Parsons HM, Wiggins CL, Stevens JL, Patt YZ. Treatment of hepatocellular carcinoma in the community: disparities in standard therapy. Liver Cancer. 2015;4:70–83.
7. Kornienko AE, Guenzl PM, Barlow DP, Pauler FM. Gene regulation by the act of long non-coding RNA transcription. BMC Biol. 2013;11:59.
8. Ponting CP, Oliver PL, Reik W. Evolution and functions of long noncoding RNAs. Cell. 2009;136:629–41.
9. Xu XF, Li J, Cao YX, Chen DW, Zhang ZG, He XJ, Ji DM, Chen BL. Differential Expression of Long Noncoding RNAs in Human Cumulus Cells Related to Embryo Developmental Potential: A Microarray Analysis. Reprod Sci. 2015;22:672–8.
10. Chalei V, Sansom SN, Kong L, Lee S, Montiel JF, Vance KW, Ponting CP. The long non-coding RNA Dali is an epigenetic regulator of neural differentiation. Elife. 2014;3:e04530.
11. Braconi C, Kogure T, Valeri N, Huang N, Nuovo G, Costinean S, Negrini M, Miotto E, Croce CM, Patel T. microRNA-29 can regulate expression of the long non-coding RNA gene MEG3 in hepatocellular cancer. Oncogene. 2011;30:4750–6.
12. He JH, Han ZP, Liu JM, Zhou JB, Zou MX, Lv YB, Li YG, Cao MR. Overexpression of Long Non-Coding RNA MEG3 Inhibits Proliferation of Hepatocellular Carcinoma Huh7 Cells via Negative Modulation of miRNA-664. J Cell Biochem. 2017;118:3713–21.
13. Zhao H, Zhang X, Frazao JB, Condino-Neto A, Newburger PE. HOX antisense lincRNA HOXA-AS2 is an apoptosis repressor in all trans retinoic acid treated NB4 promyelocytic leukemia cells. J Cell Biochem. 2013;114:2375–83.
14. Fang Y, Wang J, Wu F, Song Y, Zhao S, Zhang Q. Long non-coding RNA HOXA-AS2 promotes proliferation and invasion of breast cancer by acting as a miR-520c-3p sponge. Oncotarget.

2017;8:46090–103.

15. Liu Y, Yang Y, Wang T, Wang L, Wang X, Li T, Shi Y, Wang Y. Long non-coding RNA CCAL promotes hepatocellular carcinoma progression by regulating AP-2alpha and Wnt/beta-catenin pathway. Int J Biol Macromol. 2018;109:424–34.
16. Droop, Szarvas T, Schulz WA, Niedworok C, Niegisc h G, Scheckenbach K, Hoffmann MJ. Droop J, Szarvas T, Schulz WA, Niedworok C, Niegisc h G, Scheckenbach K, Hoffmann MJ. Diagnostic and prognostic value of long noncoding RNAs as biomarkers in urothelial carcinoma. PLoS One 2017; 12: e0176287.
17. Hu Y, Pan J, Wang Y, Li L, Huang Y. Long noncoding RNA linc-UBC1 is negative prognostic factor and exhibits tumor pro-oncogenic activity in gastric cancer. Int J Clin Exp Pathol. 2015;8:594–600.
18. Su J, Zhang E, Han L, Yin D, Liu Z, He X, Zhang Y, Lin F, Lin Q, Mao P, Mao W, Shen D. Long noncoding RNA BLACAT1 indicates a poor prognosis of colorectal cancer and affects cell proliferation by epigenetically silencing of p15. Cell Death Dis. 2017;8:e2665.
19. Shen YC, Lin ZZ, Hsu CH, Hsu C, Shao YY, Cheng AL. Clinical trials in hepatocellular carcinoma: an update. Liver Cancer. 2013;2(3–4):345–64.
20. Kalyan A, Nimeiri H, Kulik L. Systemic therapy of hepatocellular carcinoma: current and promising. Clin Liver Dis. 2015;19(2):421–32.
21. Wang M, Yu F, Li P Circular RNAs: characteristics, function and clinical significance in hepatocellular carcinoma. Cancers 10, pii: E258 (2018).
22. Fu L, Jiang Z, Li T, Hu Y, Guo J. Circular RNAs in hepatocellular carcinoma: Functions and implications. Cancer Med. 2018;7:3101–9.
23. Qiu LP, et al. The emerging role of circular RNAs in hepatocellular carcinoma. J Cancer. 2018;9:1548–59.
24. Gagliardi PA, Puliafito A, Primo L. 2017. PDK1: at the crossroad of cancer signaling pathways. Semin. Cancer Biol. 30110–30114 pii: S1044-579X(17).
25. Wang R, Zhang Q, Peng X, Zhou C, Zhong Y, Chen X, Qiu Y, Jin M, Gong M, Kong D. Stellettin B induces G1 arrest, apoptosis and autophagy in human non-small cell lung cancer A549 cells via blocking PI3K/Akt/mTOR pathway. Sci Rep. 2016;6:27071.
26. Kimmelman AC. The dynamic nature of autophagy in cancer. Genes Dev. 2011;25(19):1999–2010.

Table

Table 1 Association of circARNT2 expression with clinicopathological features of HCC patients

Characteristics	circARNT2 expression Low (n = 41)	 High (n = 41)	P
Age, y ≥ 50 Gender	21	24	0.657
Female	19	22	0. 659
Serum AFP			
≥ 20	16	22	0.268
Tumor size			
≥ 5.0 cm	14	28	0.003
TNM stage			
III/IV	8	18	0.031
Distant metastasis			
Yes	6	16	0.023

Figures

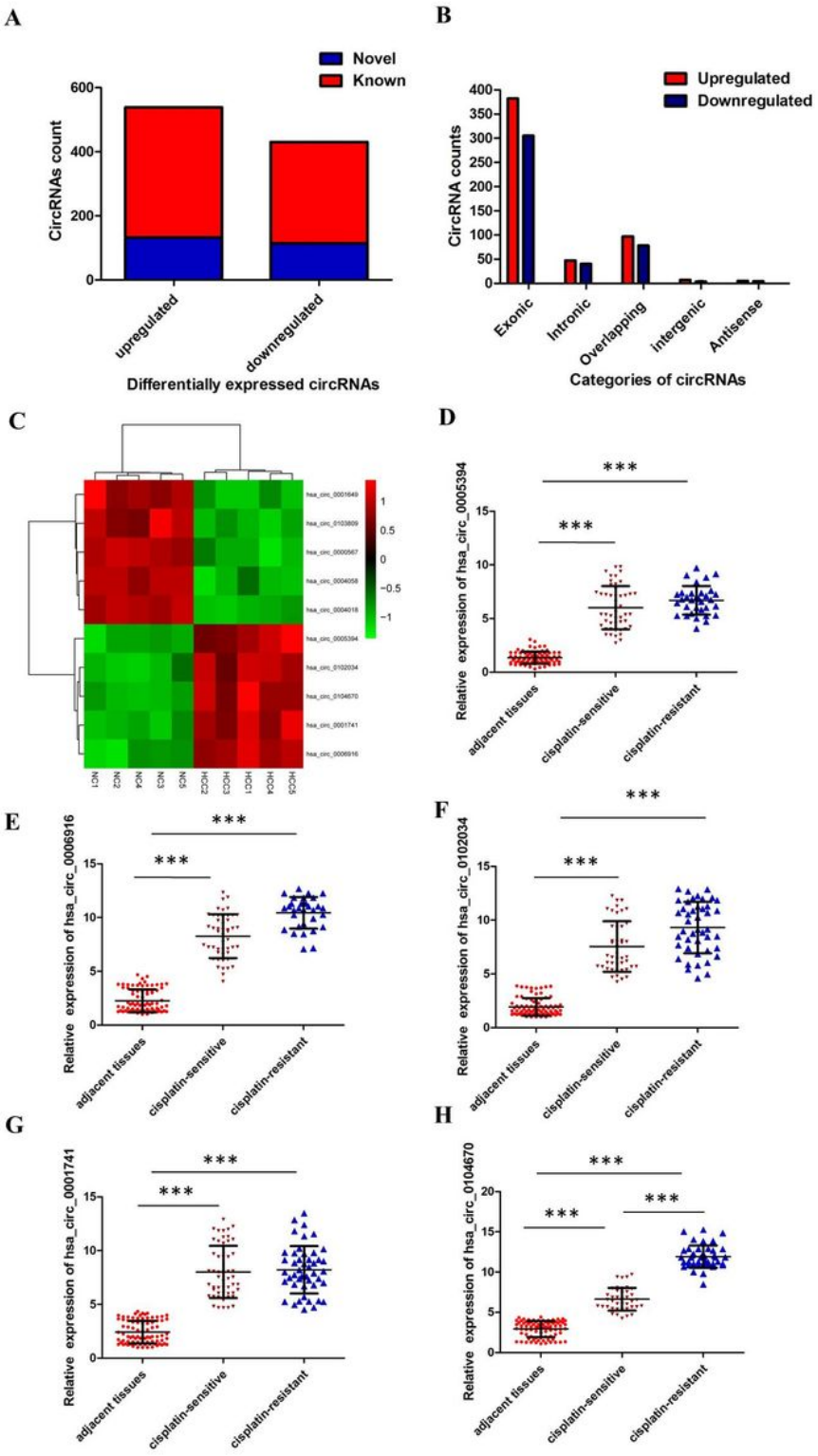

Figure 1

Upregulation of circARNT2 is associated with cisplatin resistance in HCC (A) Among the 968 differentially expressed circRNAs, 246 were verified as novel circRNAs; 722 circRNAs were identified beforehand and listed in the circRNA database; (B) The number of upregulated (red) and downregulated (green) circRNAs according to their categories of formation mode; (C) The heat map showed the top five most upregulated circRNAs and five most downregulated circRNAs between cisplatin-resistant HCC tissues and cisplatin-

sensitive HCC tissues; (D) The level of hsa_circ_0005394 was significantly increased in cisplatin-resistant HCC tissues compared with the cisplatin-sensitive tissues; (E) The level of hsa_circ_0006916 was significantly increased in cisplatin-resistant HCC tissues compared with the cisplatin-sensitive tissues; (F) The level of hsa_circ_0102034 was significantly increased in cisplatin-resistant HCC tissues compared with the cisplatin-sensitive tissues; (G) The level of hsa_circ_0001741 was significantly increased in cisplatin-resistant HCC tissues compared with the cisplatin-sensitive tissues; (H) The level of hsa_circ_0104670 was significantly increased in cisplatin-resistant HCC tissues compared with the cisplatin-sensitive tissues; All tests were at least performed three times. Data were expressed as mean ± SD. ***P < 0.001.

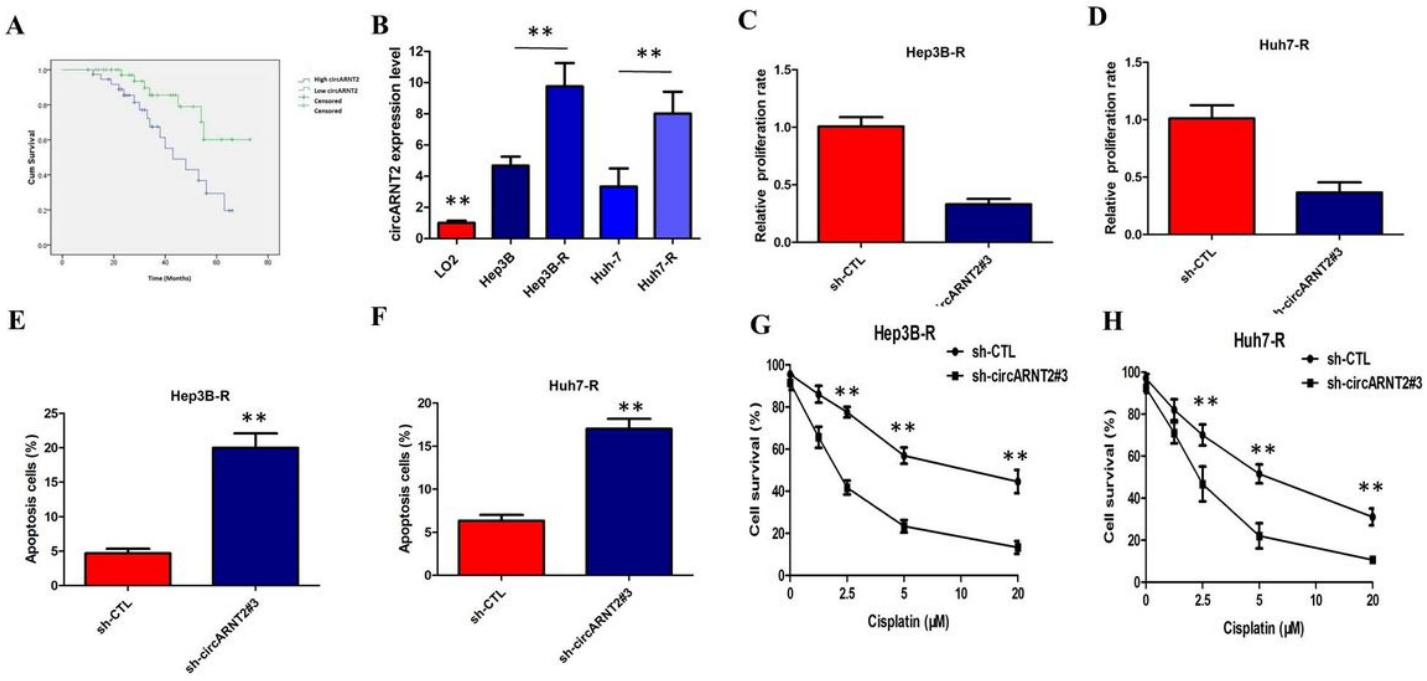

Figure 2

CircARNT2 regulates the cisplatin chemosensitivity of HCC in vitro (A) Kaplan–Meier survival analyses revealed that the HCC patients with high circARNT2 level had shorter overall survival than the patients had low circARNT2 level; (B) CircARNT2 was significantly increased in cisplatin resistant HCC cell lines (Hep3B-R and Huh7-R) compared with the parental HCC cell lines; (C) Inhibition of circARNT2 significantly inhibited cells proliferation of Hep3B-R cells; (D) Inhibition of circARNT2 significantly inhibited cells proliferation of Huh7-R cells; (E) Inhibition of circARNT2 significantly induced apoptosis of Hep3B-R cells; (F) Inhibition of circARNT2 significantly induced apoptosis of Huh7-R cells; (G) Inhibition of circARNT2 sensitized Hep3B-R cells to cisplatin; (H) Inhibition of circARNT2 sensitized Huh7-R cells to cisplatin; All tests were at least performed three times. Data were expressed as mean ± SD. **P < 0.01.

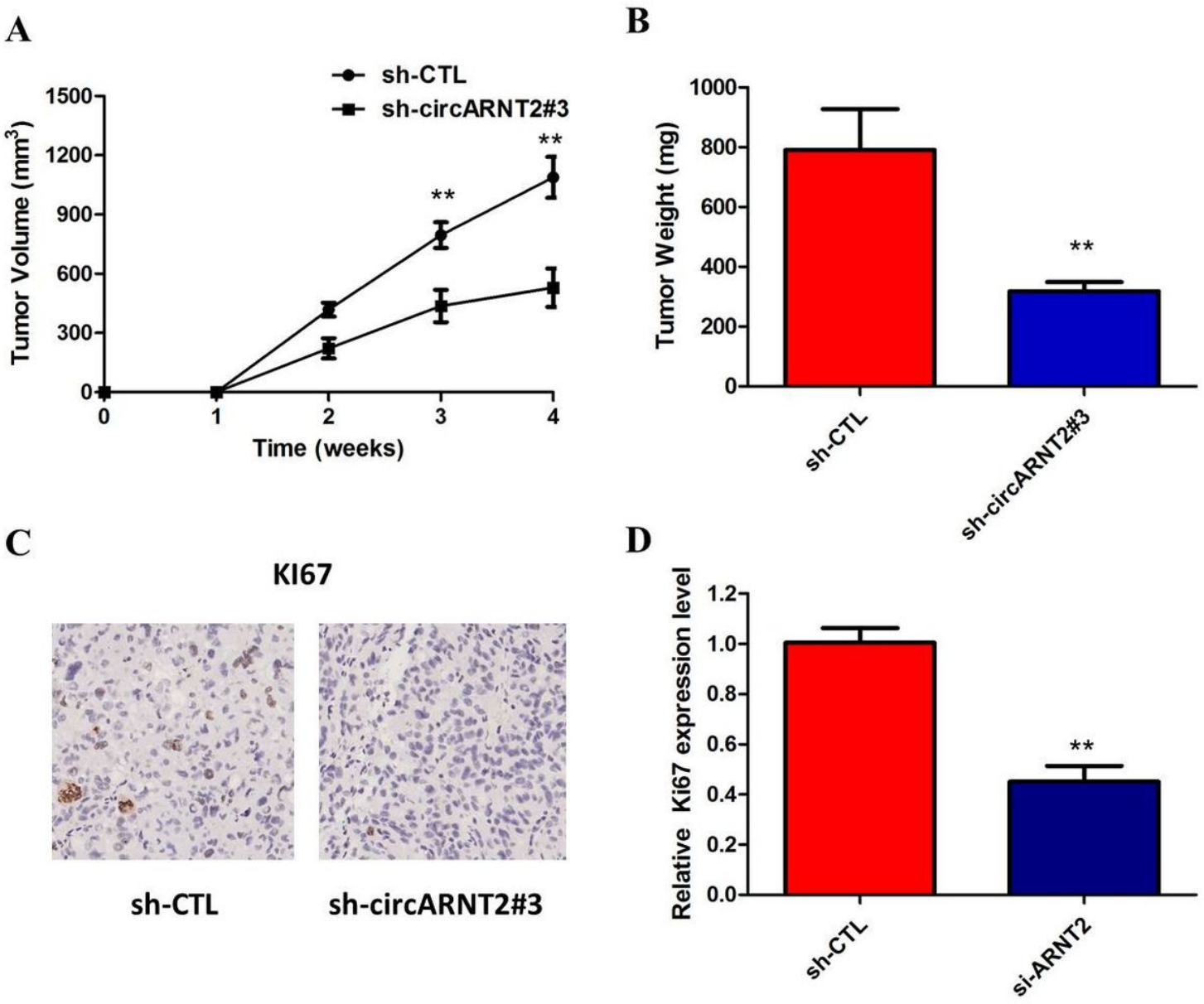

Figure 3

CircARNT2 knockdown inhibited the growth of HCC in vivo (A) The tumor volumes in nude mice injected with sh-circARNT2-transfected Hep3B-R cells were smaller than in the control nude mice; (B) Tendencies in tumor weight were consistent with those in tumor volume; (C) IHC analysis of expression levels of KI67 in xenografts; (D) The percentage of KI67- positive cells in xenografts; All tests were at least performed three times. Data were expressed as mean ± SD. **P < 0.01.

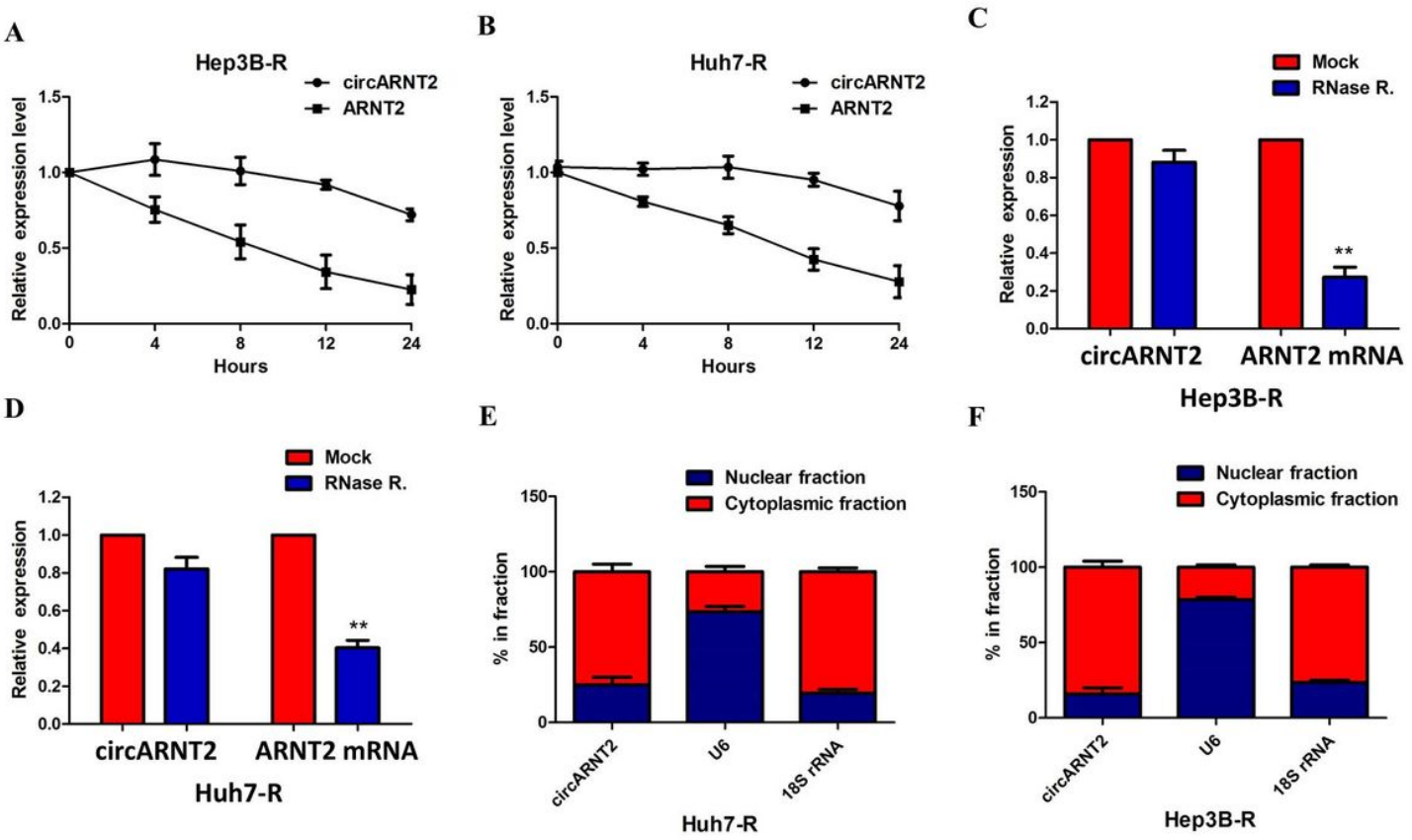

Figure 4

Confirmation of the circular structure and subcellular localization of circARNT2 A. qRT-PCR for the abundance of circARNT2 and ARNT2 in Hep3B-R cells treated with Actinomycin D at the indicated time point; B. qRT-PCR for the abundance of circARNT2 and ARNT2 in Huh7-R cells treated with Actinomycin D at the indicated time point; C. qRT-PCR for the expression of circARNT2 and ARNT2 mRNA in Hep3B-R cells treated with or without RNase R; D. qRT-PCR for the expression of circARNT2 and ARNT2 mRNA in Huh7-R cells treated with or without RNase R; E. Levels of circARNT2 in the nuclear and cytoplasmic fractions of Hep3B-R cells. F Levels of circARNT2 in the nuclear and cytoplasmic fractions of Huh7-R cells. Data are listed as means ± s.d. of at least three independent experiments. **P < 0.01.

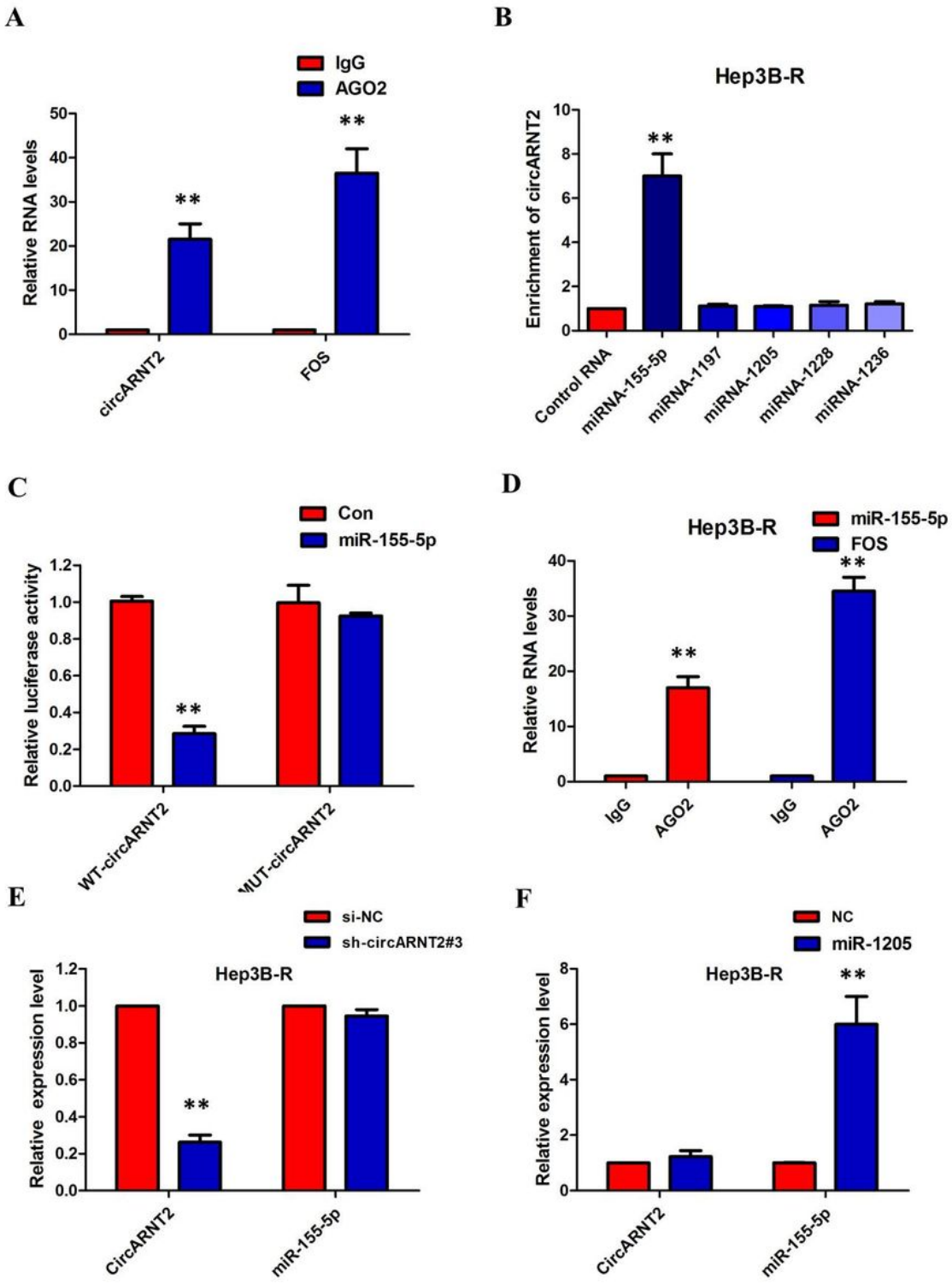

Figure 5

CircARNT2 functioned as a molecular sponge of miR-155-5p in HCC cells (A). Endogenous circARNT2 was efficiently pulled down by anti-Ago2; (B). MiRNA pull-down assay showed that circARNT2 was only efficiently enriched by miR-155-5p; (C). The luciferase reporter systems showed that miR-155-5p mimic considerably reduced the luciferase activity of the WT-circARNT2 luciferase reporter vector compared with negative control, while miR-155-5p mimic did not pose any impact on the luciferase activity of MUT-

circARNT2-transfected cells; (D). circARNT2 and miR-155-5p simultaneously existed in the production precipitated by anti-AGO2; (E). Silencing of circARNT2 did not affect the expression of miR-155-5p; (F). Transfection of miR-155-5p mimics did not affect the expression of circARNT2; All tests were at least performed three times. Data were expressed as mean ± SD. **P < 0.01.

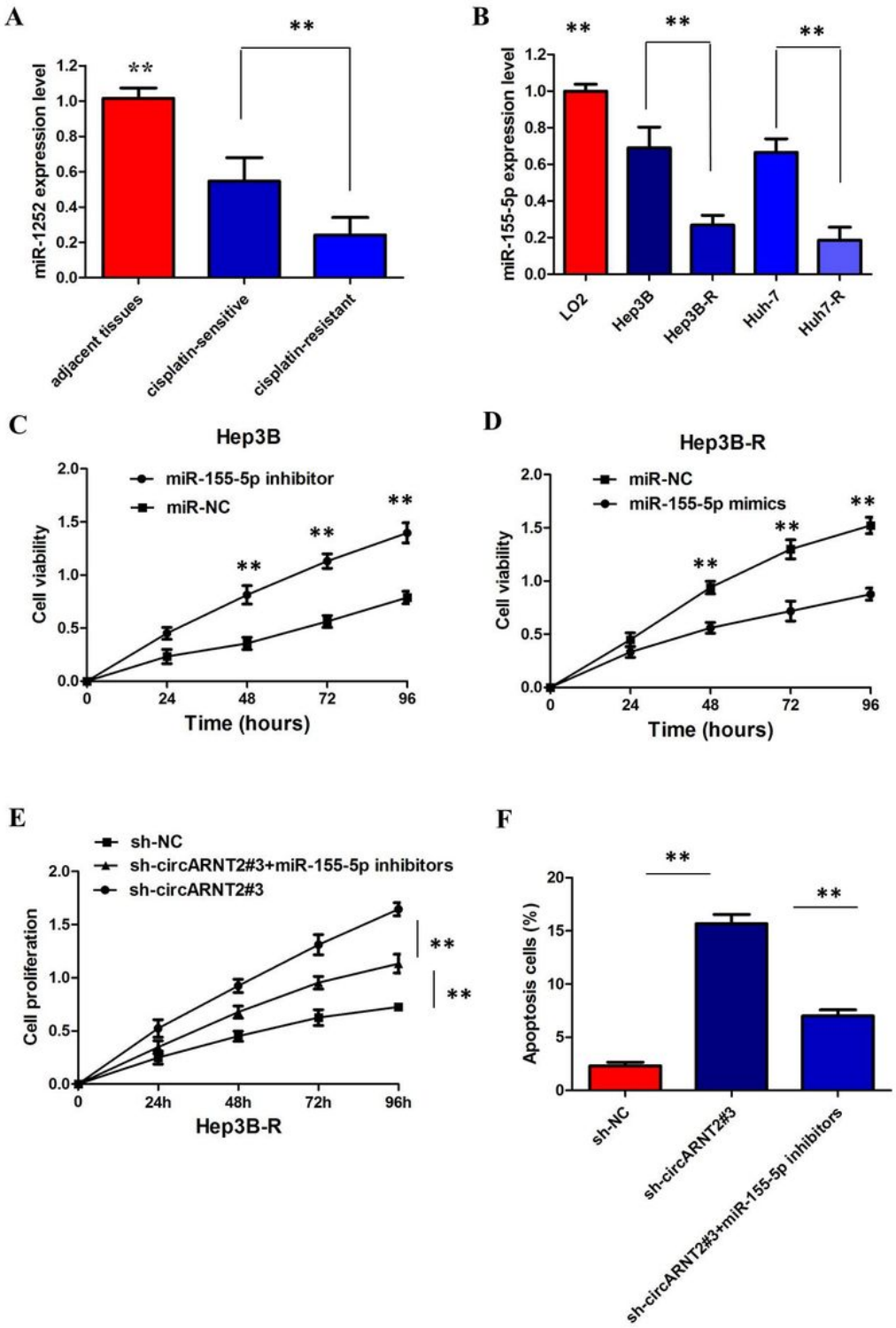

Figure 6

MiR-155-5p suppressed cisplatin-resistant HCC tissues resistance of HCC cells (A). The level of miR-155-5p was significantly decreased in cisplatin-resistant HCC tissues; (B). The level of miR-155-5p was significantly decreased in cisplatin resistant cells than that in cisplatin sensitive cells; (C). Hep3B cells transfected with miR-155-5p inhibitors grew at a dramatically higher rate as compared with controls; (D). miR-155-5p mimics markedly inhibits the cell growth in Hep3B-R cells when compared with cells transfected with miR-NC; (E). Downregulation of circARNT2-induced decrease of cell growth was partially restored by miR-155-5p inhibition; (F). Downregulation of circARNT2-triggered apoptosis was attenuated after cotransfected with miR-155-5p inhibitor; All tests were at least performed three times. Data were expressed as mean ± SD. **P < 0.01.

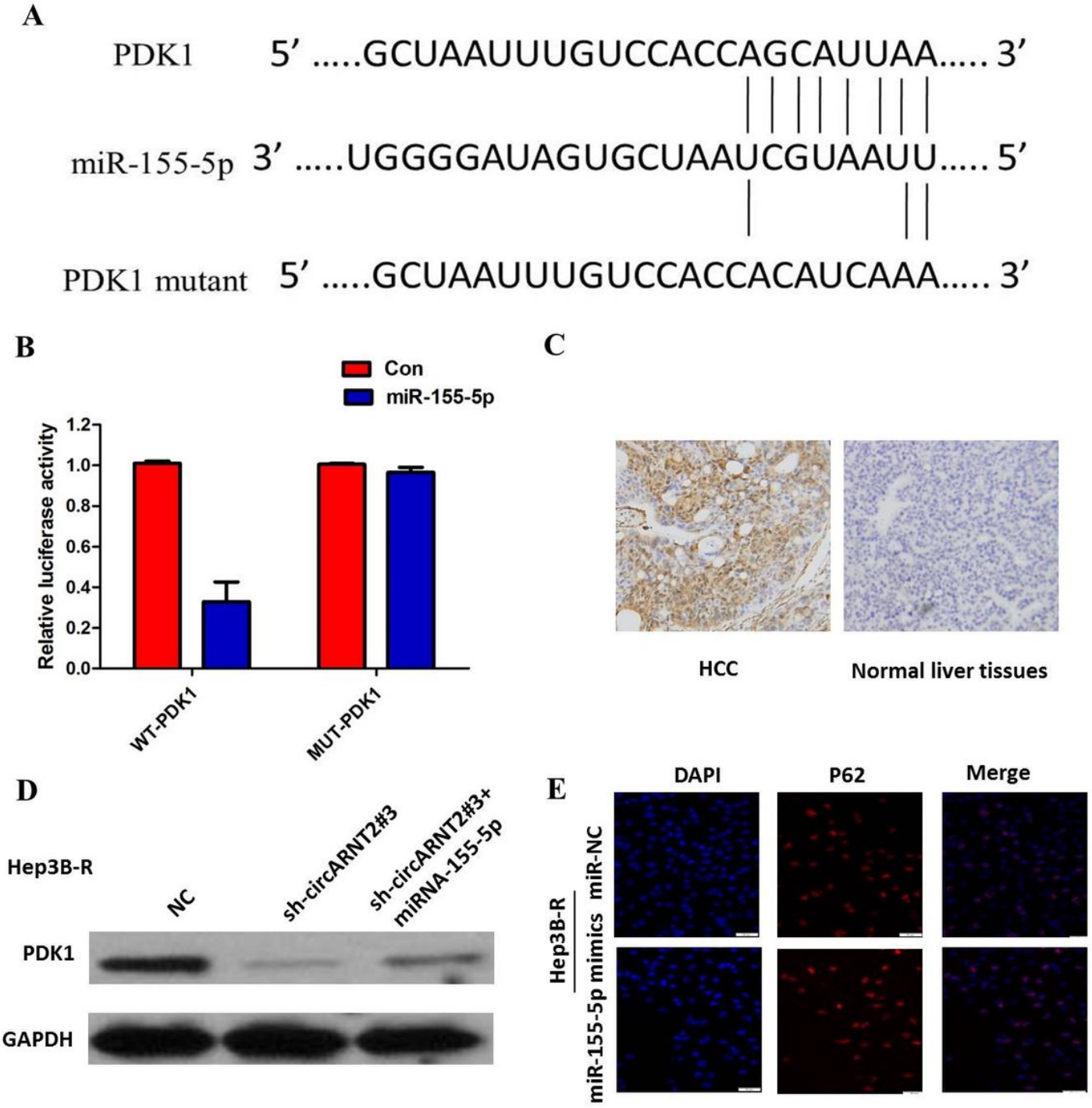

Figure 7

MiR-155-5p inhibits PDK1 and promotes autophagy (A) Bioinformatics analysis revealed the predicted binding sites between miR- 155-5p and PDK1; (B) Luciferase reporter assay demonstrated miR- 155-5p mimics significantly decreased the luciferase activity of PDK1-wt in HCC cells; (C) The immunohistochemistry results showed that PDK1 expression in HCC specimens was significantly upregulated compare with that in the adjacent normal tissues; (D) The western blotting assay showed that inhibition of circARNT2 mediated decrease of PDK1 protein expression was significantly recuperated following miR-155-5p inhibitors; (E) The immunofluorescence assay showed that the expression levels P62 was significantly reduced in miR-155-5p-overexpressing cells compared to the corresponding control cells.

Supplementary Files

This is a list of supplementary files associated with this preprint. Click to download.

- figS1.jpg
- figS1.jpg
- figS1.jpg
- data1.pdf
- data1.pdf
- data1.pdf